The prototype of the GOPI engine is developed based on the mathematical modeling and tested for various conditions and materials. Simulation and experimental investigations are done to validate the theory and the mathematical modeling.

4.1 Analysis with ANSYS

The finite elements of two are package ANSYS is used for investigation of the magnetic field components properties. This tool includes three stages: preprocessor, solver and postprocessor. The procedure for carrying out a static magnetic analysis consists of following main steps: create the physics environment, build and mesh the model, as sign physics attributes to each region within the model, apply boundary conditions and loads (excitation), obtain the solution, and review the results (ANSYS Documentation).

A typical magnetic field problem is described by defining its geometry, material properties, currents, boundary conditions, and the field system equations. The computer requires the input data and provides the numerical solution of the field equation and the output of desired parameters. If the values are found unsatisfactory, the design is modified and parameters are recalculated. The process is repeated until optimum values for the design parameters are obtained.

In order to define the physics environment for an analysis, it is necessary to enter in the ANSYS preprocessor (PREP7) and to establish a mathematical simulation model of the physical problem. In order to create this environment, the following steps are presented below: set GUI Preferences, define the analysis title, define the element types and options, define the element coordinate systems, set real constants and define a system of units, and define the material properties (ANSYS Documentation).

The Global Cartesian coordinate system is the default. A different coordinate system can be specified by the user by indicating its origin location and orientation angles. The coordinate system types are Cartesian, Cylindrical (circular or elliptical), Spherical, and Toroidal.

Some materials with magnetic properties are defined in the ANSYS material library. The materials can be modified to correspond more closely to the analyzed problem and to be loaded in the ANSYS database. The copper property shows temperature which depends on resistivity and relative permeability. All other properties are described in terms of *B-H* curves. Most of the materials included in ANSYS are used for modeling the electromagnetic phenomenon. The element types are used to establish the physics of the problem domain. Some element types and options are defined to represent the different regions in the model. If some laminated materials are aligned in an arbitrary form, the element coordinate system or systems have to be identified and used. The applications presented in this chapter use the PLANE53 element in the two-dimensional problem and the SOLID97 element for the three-dimensional problem.

In order to obtain the magnetic field values, the Maxwell's equations are solved by using the input data. The nodal values of the magnetic vector potential are considered as main or primary unknowns. Their derivatives (e.g., flux density) are the secondary unknowns. After this, it is possible to choose the type of solver to be used. The available options include Sparse solver (default) , Frontal solver, Jacobi Conjugate Gradient (JCG) solver, JC Gout-of- memory solver, Incomplete Cholesky Conjugate Gradient (ICCG) solver, Preconditioned Conjugate Gradient solver (PCG), and PCG out-of-memory solver (ANSYS Documentation). Finite element analysis is often used to calculate the magnetic field in devices such as, power generators, transformers, video display devices and so forth. FEA package (ANSYS14.0, ANSYS 11.0) is used to analyse the magnetic characteristics of the GOPI engine.2Dmagnetic static analysis is used to determine the magnetic field and gate behavior caused by the permanent magnets and magnetic shield material.
The aims behind the magnetic analysis are:

1) To determine the magnetic field patterns of the permanent magnet at the static position,

2) To investigate the distribution of the magnetic flux across the gate when the gate is in neutral mode,

3) To determine the magnetic flux distribution across the gate when the gate is in active mode,

4) To determine the maximum approach distance of the magnetic piston,

5) To determine total available force at piston head,

6) To determine attachment of the gate with m_1& m_2,

7) Force required for pulling the gate from neutral position and

8) Efficiency of the engine.

The model comprises of a gate, permanent magnets and the surrounding air. A two dimensional model is constructed to investigate the optimal configuration.

4.2 Magnet(s) in Air Medium

In ANSYS simulation, the 2Delement PLANE13 (2Dcoupledfieldsolid,4-nodewith four degree of free do m per node) was applied to all interior regions of the model, including the permanent magnet region, the gate region and considerable region of the surrounding space, while the edge of the whole model is modeled by INFINI10 element to simulate an infinite extension of the surrounding air. Because the elements are two dimensional, each node has only one vector potential degree of freedom AZ (vector potential in Z direction).The INFINI 10 element has non- linear magnetic capabilities for modeling B-H curves or permanent magnet demagnetization curves.

4.2.1 One Magnet

When the magnet placed in air medium, the magnetic flux lines coming out from North Pole will enter into the South Pole and will flow in closed loop. The contour lines shown in the figure4.1 indicates the flux density at a particular point. From the figure 4.2. it can be observed that the magnetic field has maximum intensity in the center and reduces gradually in the radial direction. The geometry of the chosen magnet is circular solid cylinder of 10mm thick and 60mm diameter and having magnetic flux intensity at center is 1.2 T if measured much closer to the center. From the fig4.1& fig 4.2, the intensity of magnetic field near center is 1.02 T and at the edge is it only 0.567 T, almost half of the center. It is because of the open circuit, the magnetic flux intensity available at center is about 85% of the rated value.

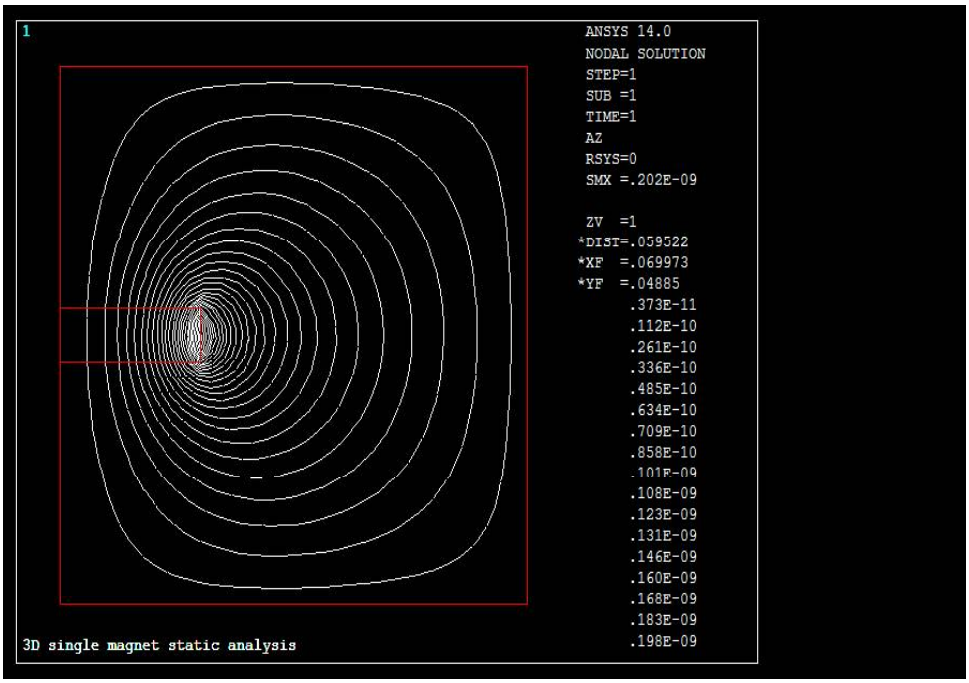

Figure 4.1: Magnetic contour lines in air medium

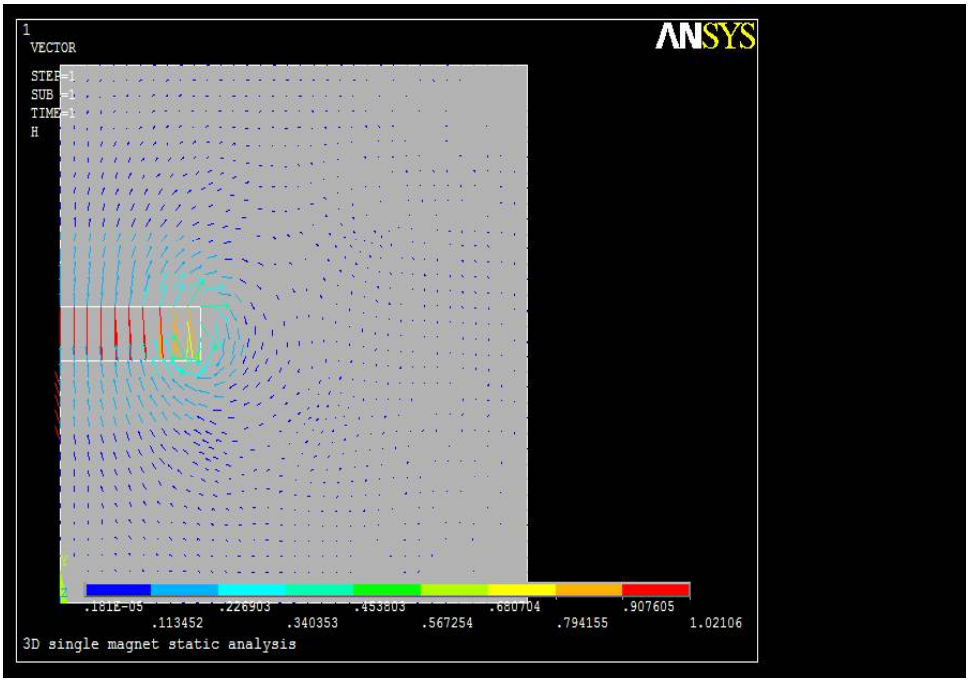

Figure 4.2: Magnetic field intensity in air medium

The variation in magnetic field along its radial direction is tabulated in the table 4.1; from this table, it can be seen that around 75% of the rated magnetic field is available in less than 50% area of the magnet.

Table 4.1: Magnetic field intensity and distance relation for a permanent magnet

Sr. No	Distance from center(mm)	Magnetic field intensity(T)
1	0.0	1.020
2	0.022	0.907
3	0.025	0.794
4	0.026	0.680
5	0.030	0.567

4.2.2 Two Magnets

When two magnets placed in air medium, when opposite poles of the magnets are facing they attract and vice versa. As the maximum flux intensity is at the center, the maximum intensity of the force will be at the center. As the distance between the magnets increases the magnetic field between the magnets reduces drastically as shown in the table4.2

Table 4.2: Force at the center of two magnets for various distances (H=1.2 T)

Sr. No	Y-separation between the magnets(mm)	Force between two magnets(N)
1	10	178200
2	20	26325
3	30	7614
4	60	752.4
5	120	61.87

The magnetic circuit contour lines between the two magnets & gate and the magnetic field intensity are represented in the figure 4.3 (a, b, c, d).

4.2.3 Magnet and Gate in Air Medium

When a magnetic material placed between these magnets, all magnetic flux lines will intend to pass through the material to complete the magnetic circuit. The high permeable gate when placed between the m_1 and m_2, it will complete magnetic circuit

with m_1 and m_2; as the flux lines coming from the magnets will start passing through the gate as shown in the figure 4.3 (c). The intensity of attachment of the gate with m_1 and m_2 is high at edges as these are open ends of the magnetic circuit and hence magnetic flux intensity increases, as shown in the figure 4.3(d).

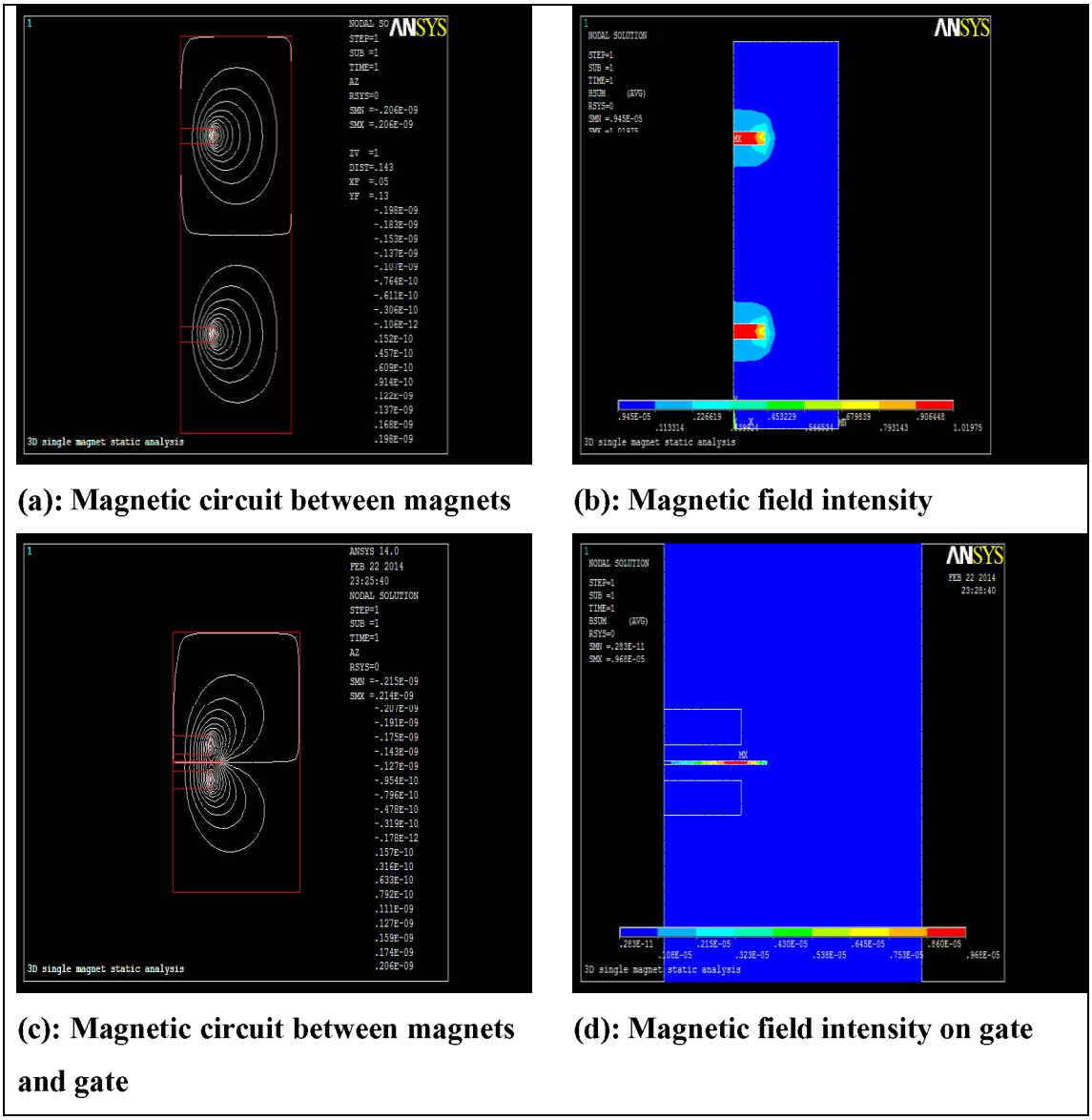

(a): Magnetic circuit between magnets

(b): Magnetic field intensity

(c): Magnetic circuit between magnets and gate

(d): Magnetic field intensity on gate

Figure 4.3: Magnetic Circuit between magnets & gate and field intensity

4.3 Static Analysis of GOPI Engine for 1 mm of Gate Thickness

The working of the GOPI engine depends upon the shield properties of the gate. It is one of the major objectives of the study to find out dependency of gate's working on the permeability of the material selected for the gate development, the distance of the

gate from m_1& m_2 and thickness of the gate. It is observed that if the m_1 and m_2 are placed at a long distance (more than their diameter), the magnetic effect between them will become very weak. So the m_1 and m_2 are placed at a distance of 60 mm, 30 mm, 20 mm, 10 mm to find out the behavior of the gate and magnet system.

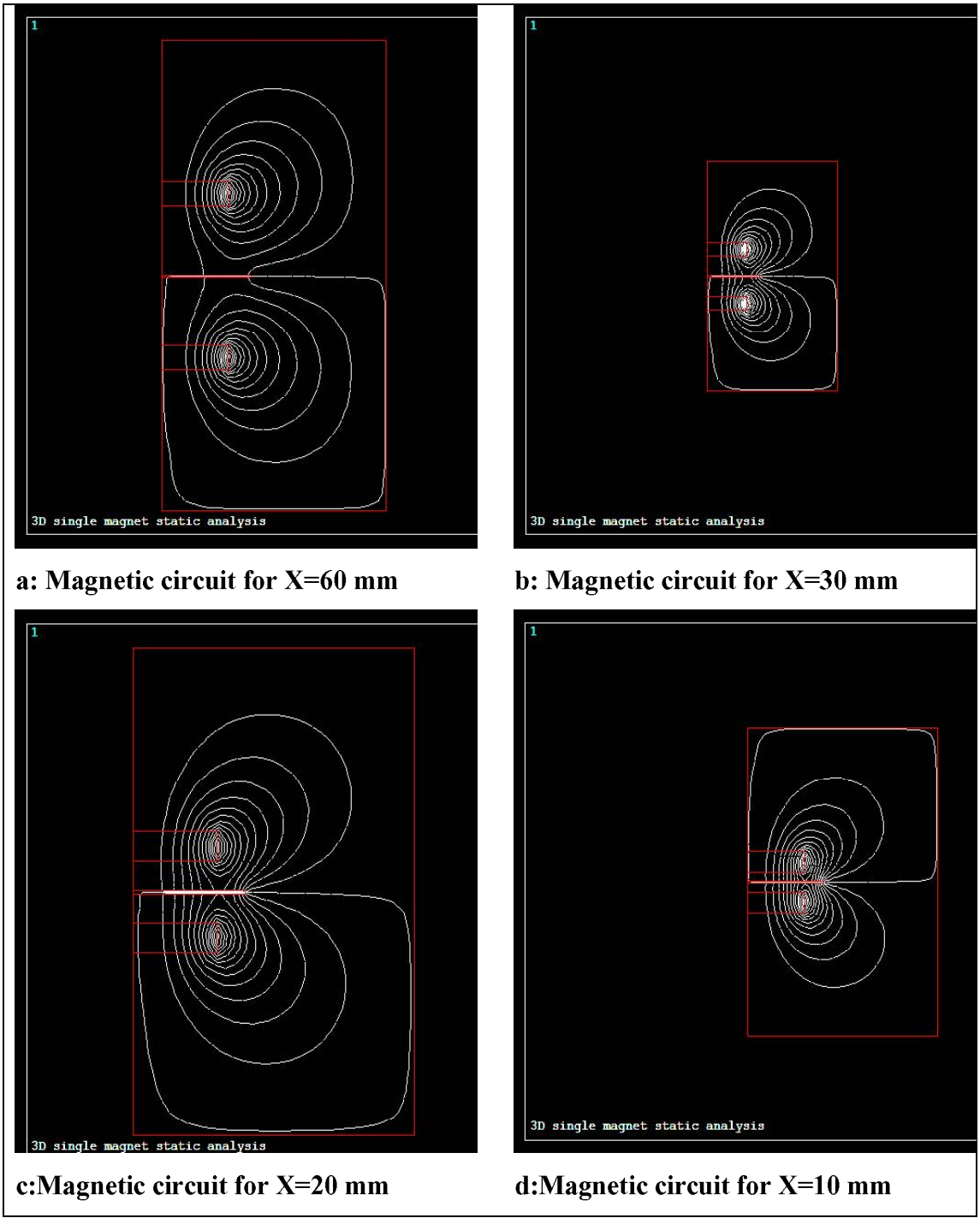

a: Magnetic circuit for X=60 mm

b: Magnetic circuit for X=30 mm

c:Magnetic circuit for X=20 mm

d:Magnetic circuit for X=10 mm

Figure 4.4: Magnetic circuit contour lines for variable distance and t_1=1mm, μ_1=30

For simulation purpose, two different thicknesses of the gate are chosen as t_1=1mm and t_2=2mm. The test was run for three different permeability of the gate as μ_1= 30k,

μ_2=100k and μ_3=300k. In all static analysis, the gate is kept at the midway of the m_1 and m_2. The distance between the m_1 and m_2 is from center to center of the magnets. The magnetic behavior of gate and the magnets are studies and summarized in the figure 4.4. The results obtained for gate thickness t_1=1mm for permeability ranging from 30k to 300k and for different distance ranging from 60mm to 10 mm are presented in the fig 4.4 (a, b, c, d).

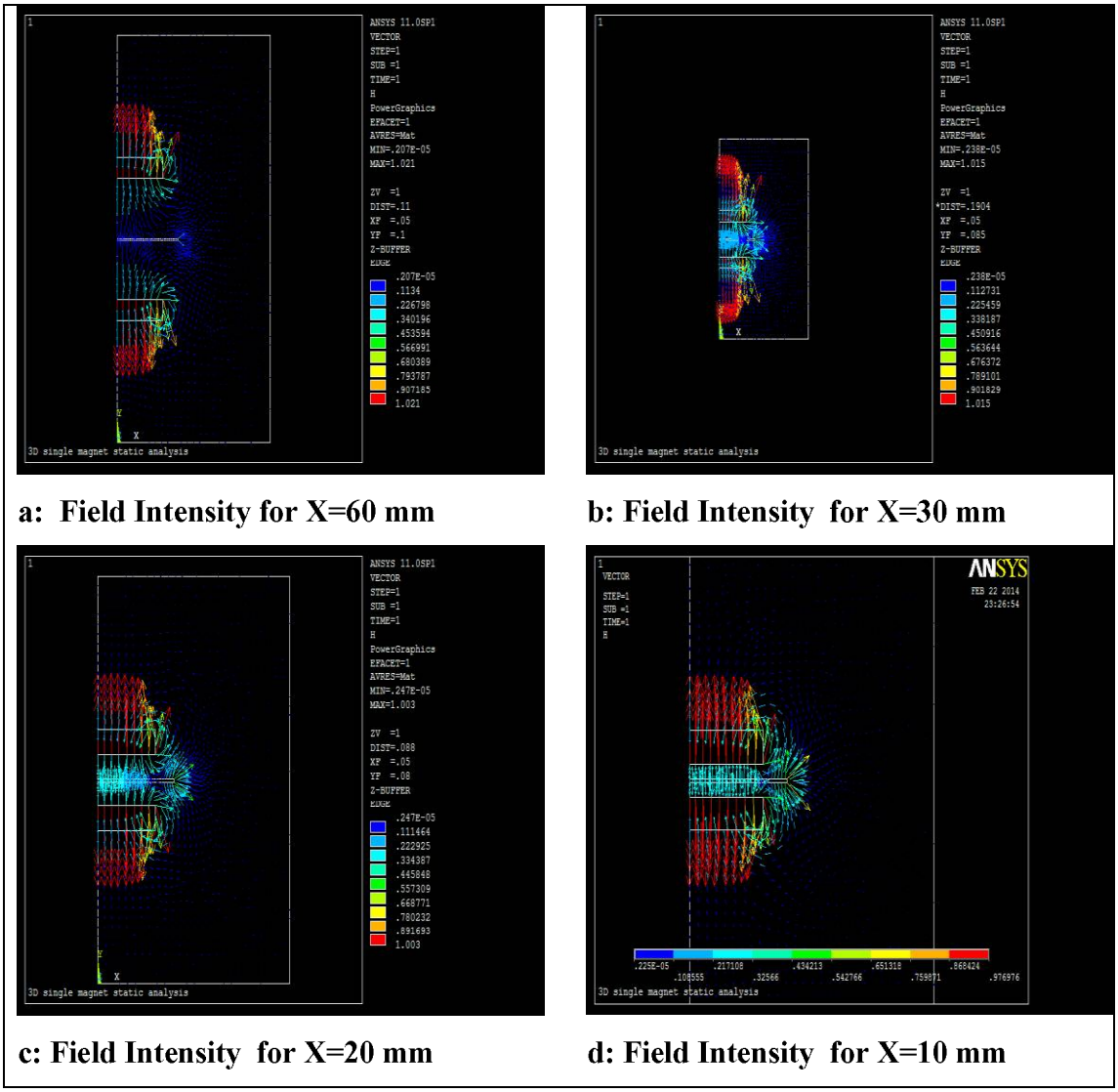

a: Field Intensity for X=60 mm

b: Field Intensity for X=30 mm

c: Field Intensity for X=20 mm

d: Field Intensity for X=10 mm

Figure 4.5: Magnetic field intensity at gate center for different distance and t_1=1mm, μ_1=30k

As the distance between the m_1& m_2 increase, the force between them decreases, as shown in the figure 4.5. As the permeability of the gate increase, the field blocked by the gate for same location will increase compared to that of less permeable value of the gate. The result obtained for the t_1=1mm, μ_2=100k for Y =60mm, 30mm, 20 mm,

10 mm are presented in the figure 4.6. From the fig 4.6 (a, b, c, d), it can be observed that as the distance between the gate and the magnets is minimum, the maximum flux passes through the magnetic circuit.

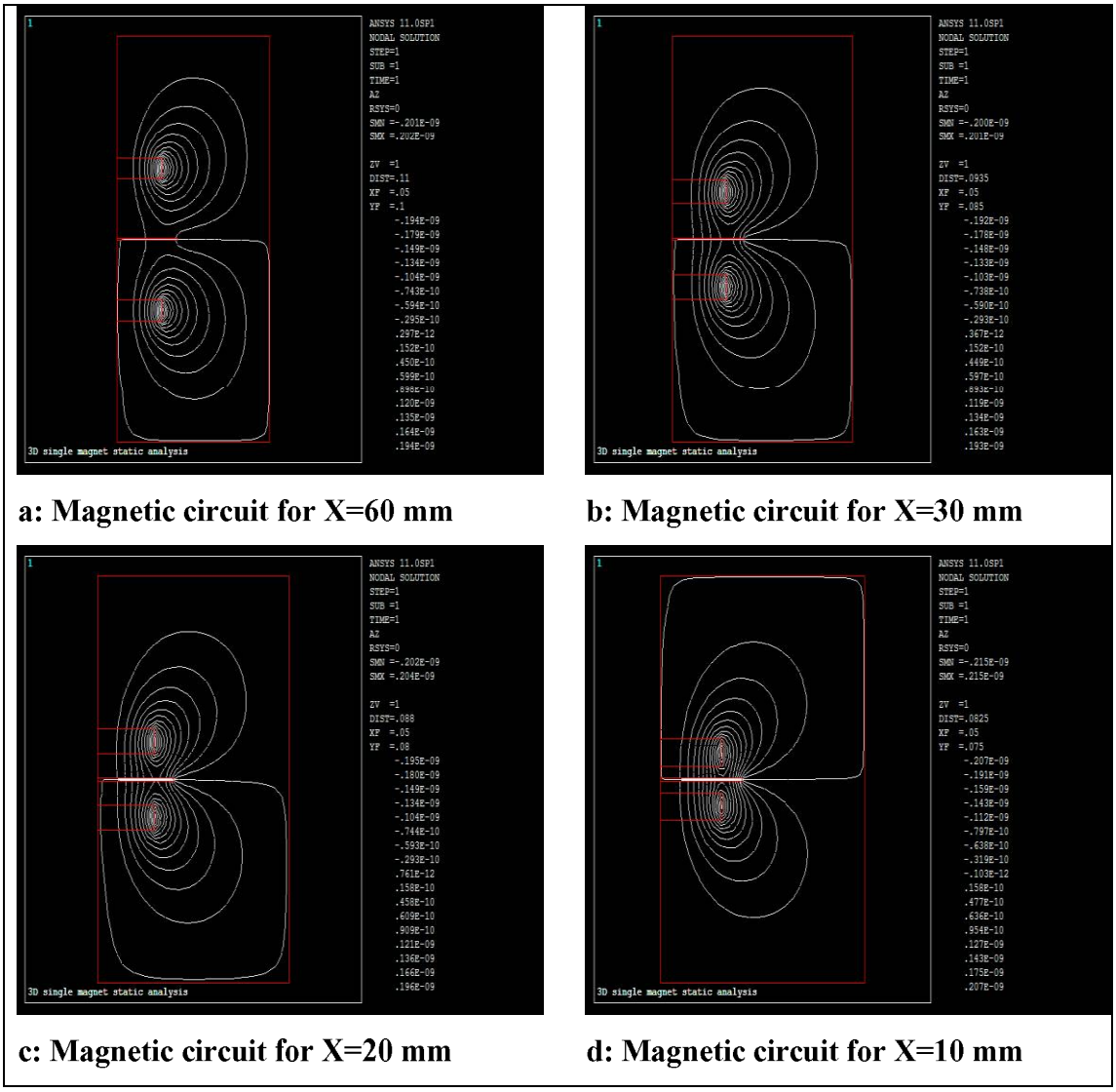

a: Magnetic circuit for X=60 mm

b: Magnetic circuit for X=30 mm

c: Magnetic circuit for X=20 mm

d: Magnetic circuit for X=10 mm

Figure 4.6: Magnetic circuit contour lines for variable distance and t_1=1mm, μ_2=100k

The magnetic field intensity for the t_1=1mm, μ_2=100k for Y =60mm, 30mm, 20 mm, 10 mm are presented in the figure 4.7. It is observed that the field intensity is maximum at the gate for minimum distance between the gate and the magnets. The gate virtually attached strongly with the magnets. More force is required to pull the gate from the neutral position to produce the power stroke.

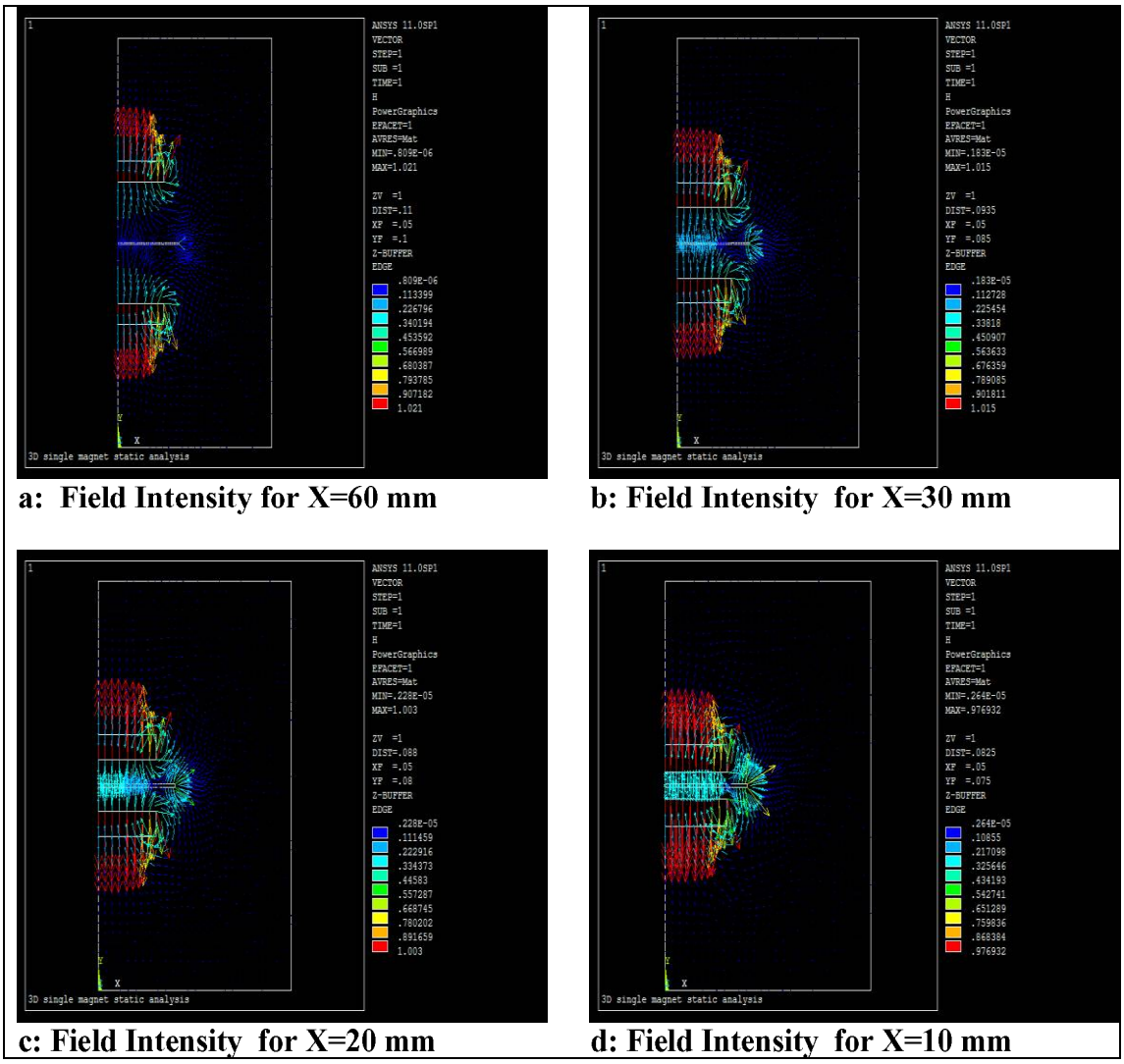

a: Field Intensity for X=60 mm

b: Field Intensity for X=30 mm

c: Field Intensity for X=20 mm

d: Field Intensity for X=10 mm

Figure 4.7: Magnetic field intensity at gate center for different distance and t_1=1mm, μ_2=100k

As the permeability of the gate increase, the field retained by the gate for same location will increase compared to that of less permeable value of the gate. The result obtained for the t_1=1mm, μ_3=300k for Y =60mm, 30mm, 20 mm, 10 mm are presented in the figure 4.8.The shielding effect of the gate for μ_1=30k, μ_2=100k and μ_3=300k increases as the distance between the magnets is reduced.

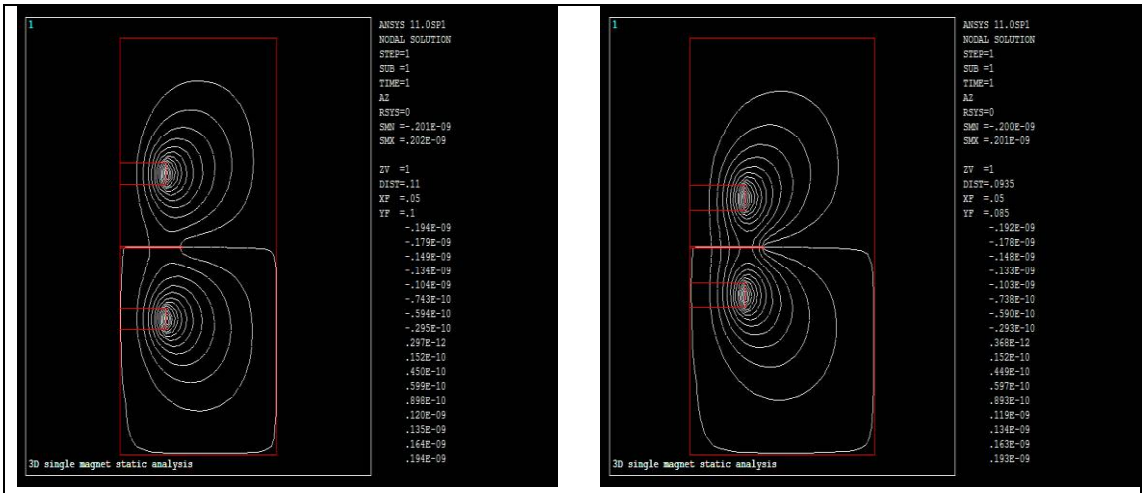

a: Magnetic circuit for X=60 mm

b: Magnetic circuit for X=30 mm

c: Magnetic circuit for X=20 mm

d: Magnetic circuit for X=10 mm

Figure 4.8: Magnetic circuit contour lines for variable distance and t_1=1mm, μ_3=300k

The magnetic field intensity for the t_1=1mm, μ_3=300k for Y =60mm, 30mm, 20 mm, 10 mm are presented in the figure 4.9. The gate virtually attached strongly with the magnets compared to less permeable gate. The magnetic field retained by the gate is maximum for μ_3=300k but at the same time, more magnetic inertia force is required to produce the power stroke.

The value of the field blocked by the gate decreases as the distance between the m_1 and m_2 increases. The variation in the field blocked by the gate with different location of the gate for μ_1=30k, μ_2=100k, , μ_3=300k, and for the distances of 60mm, 30mm, 20mm, and 10mm between the magnets is presented in the table 4.3.

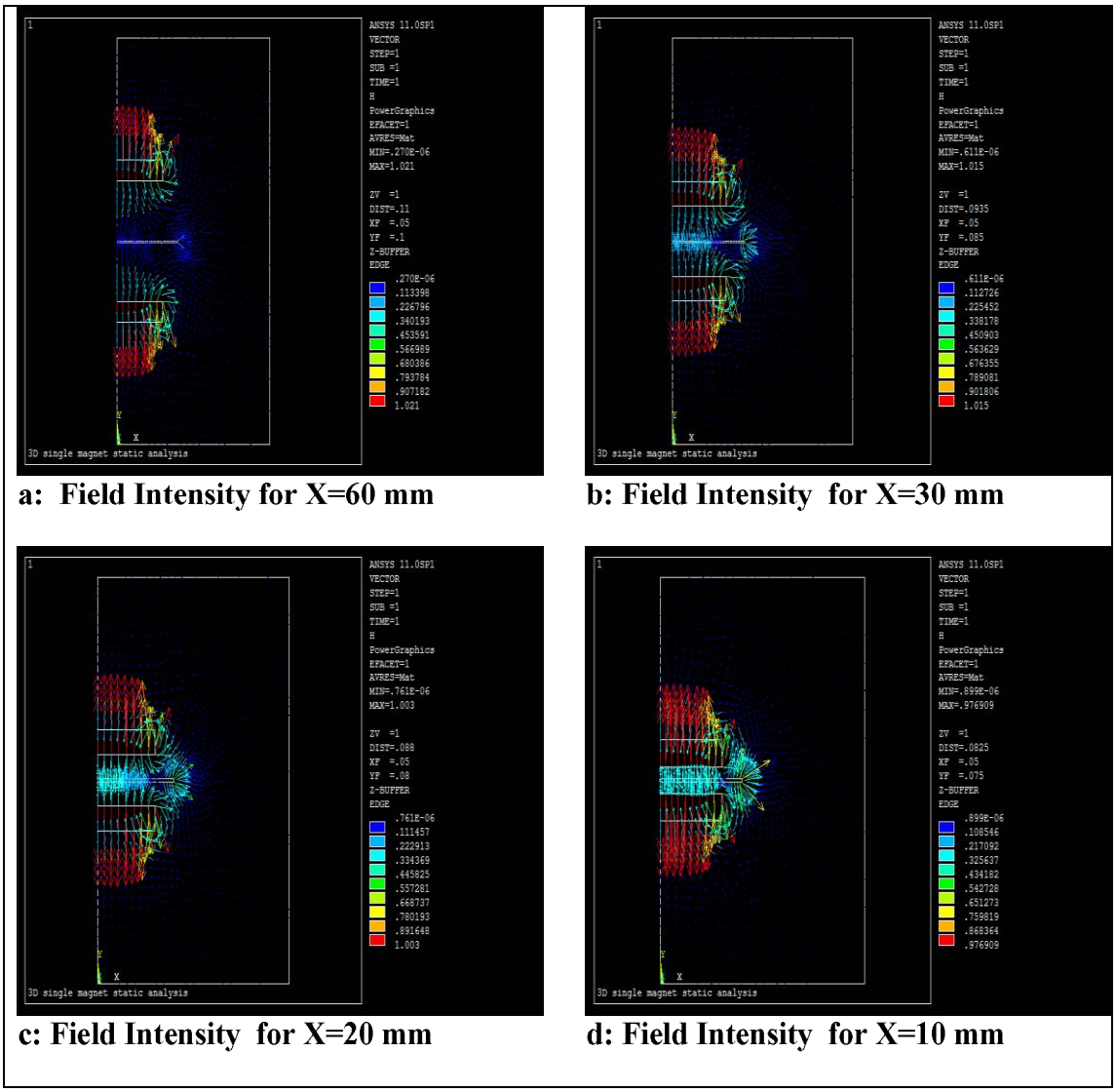

a: Field Intensity for X=60 mm

b: Field Intensity for X=30 mm

c: Field Intensity for X=20 mm

d: Field Intensity for X=10 mm

Figure 4.9: Magnetic field intensity at gate center for different distance and t_1=1mm, μ_3=300k

From the table 4.3, it can be concluded that the shielding effect of the gate increase as the permeability of the gate material and hence both the magnets can be brought closer to each other by applying less potential energy of the system. As the working of the GOPI engine entirely depends upon the gate, it can be observed that the GOPI engine will work efficiently when high permeable material chosen for gate development.

Table 4.3: Magnetic field shielding for t=1mm and different permeability and distance

Sr No	Distance/ Permeability	μ_1=30k	μ_2=100k	μ_3=300k
		Field blocked by gate (T)		
1	5	0.23	0.55	0.77
2	10	0.11	0.24	0.43
3	15	0.03	0.11	0.21
4	30	0.207e-5	Not applicable	Not applicable

4.4 Static Analysis of GOPI Engine for 2 mm Gate Thickness

As the thickness of the gate affects the working performance of the gate, so a simulation is repeated for thickness of the gate for t_2=2mm under the same conditions. As it is observed that the GOPI engine will perform better when the distance between the m_1 and m_2 is less. So the simulation for t_2=2mm is run for 20 mm and 10mm center to center distance between the m_1 and m_2.

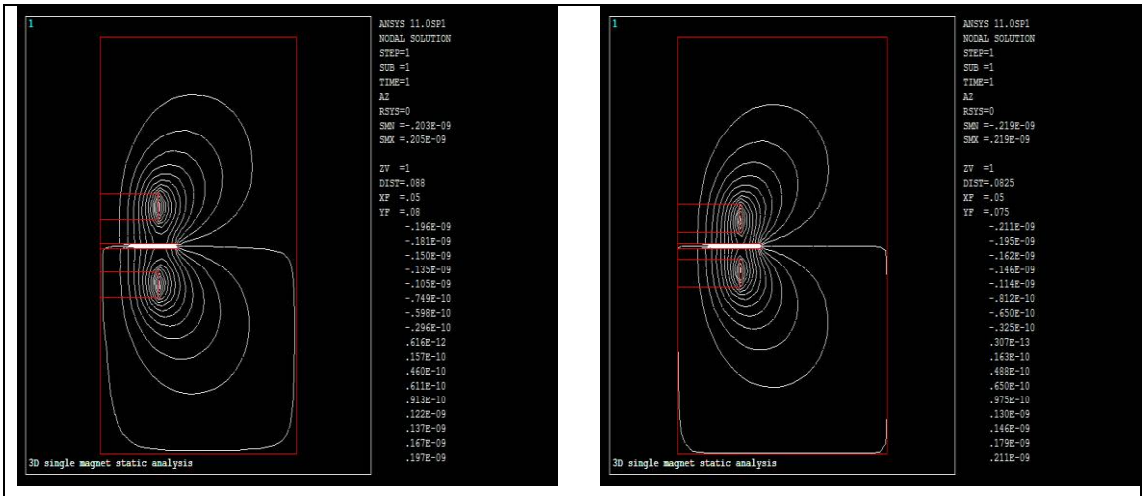

a: Magnetic circuit for X=20 mm **b: Magnetic circuit for X=10 mm**

Figure 4.10: Magnetic circuit contour lines for variable distance and t_2=2mm, μ_1=30k

The results obtained for gate thickness t_2=2mm, for permeability for 30k and for different distance of 20 mm and 10 mm, are presented in the figure 4.10. As the thickness of the gate increases, the field blocked by the gate for same location will increase as compared to less thickness of the gate.

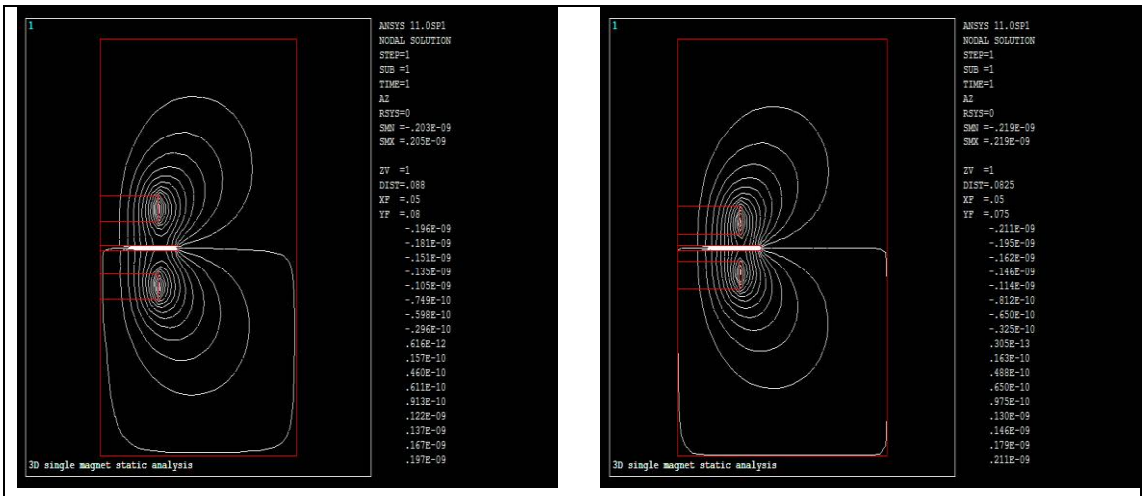

a: Magnetic circuit for X=20 mm **b: Magnetic circuit for X=10 mm**

Figure 4.11: Magnetic circuit contour lines for variable distance and t_2=2mm, μ_2=100k

The results obtained for gate thickness t_2=2mm for permeability of 100k and 300k and for distances of 20 mm and 10 mm are presented in the figure 4.11 and figure 4.12 respectively.

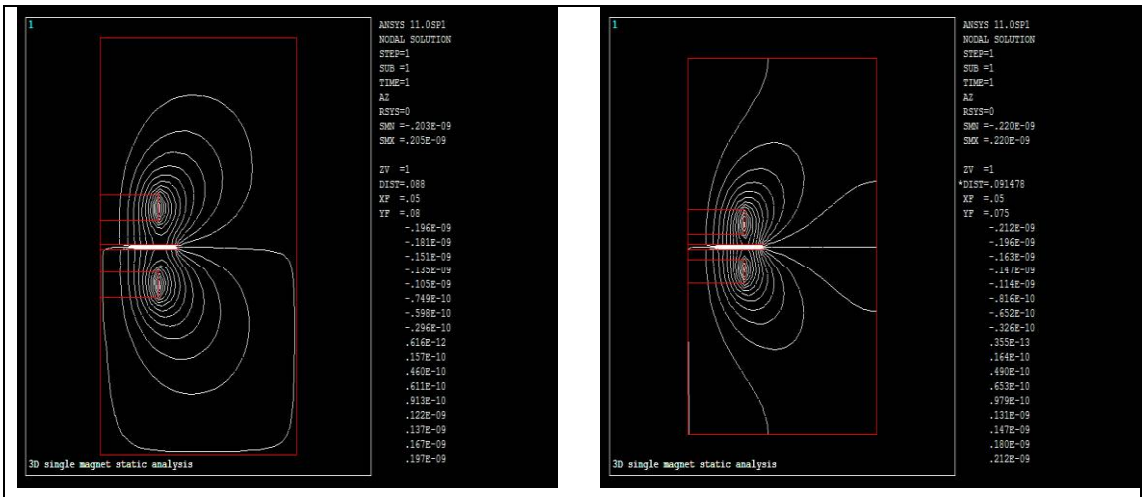

a: Magnetic circuit for X=20 mm **b: Magnetic circuit for X=10 mm**

Figure 4.12: Magnetic circuit contour lines for variable distance and t_2=2mm, μ_3=300k

The magnetic field intensity for the t_2=2mm, μ_1=30k μ_2=100k μ_3=300k for Y distances of 20 mm, 10 mm are presented in the figure 4.13, figure 4.14 and figure 4.15 respectively. The gate virtually attached strongly with the magnets compared to

less thickness of it. The magnetic field retained by the gate is maximum for μ_3=300k.

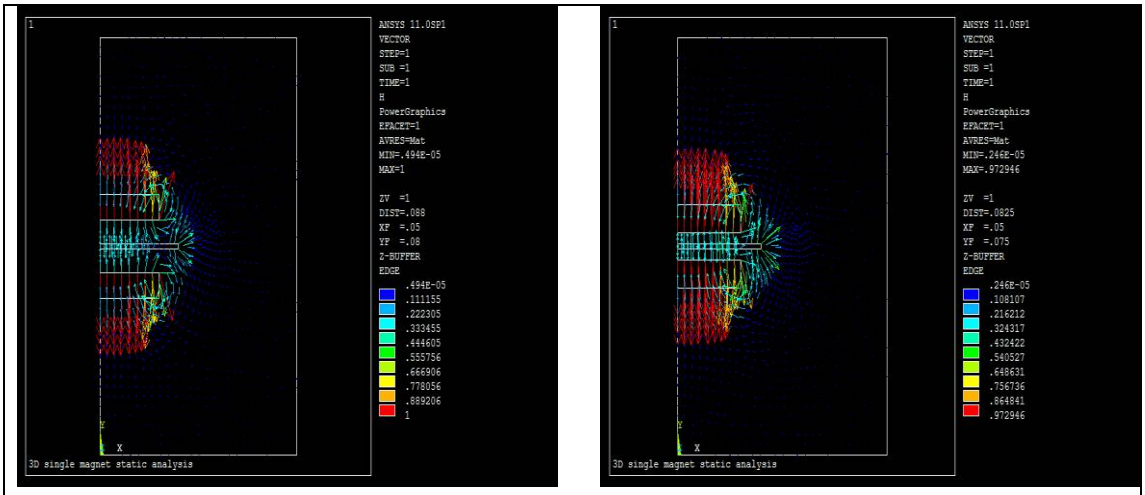

a: Field Intensity for X=20 mm **b: Field Intensity for X=10 mm**

Figure 4.13: Magnetic field intensity at gate center for different distance and t_2=2mm, μ_1=30k

It can be observed from the fig .13 to fig 4.15 that the flux density at the center of the gate is maximum when the permeable value of the gate material is high.

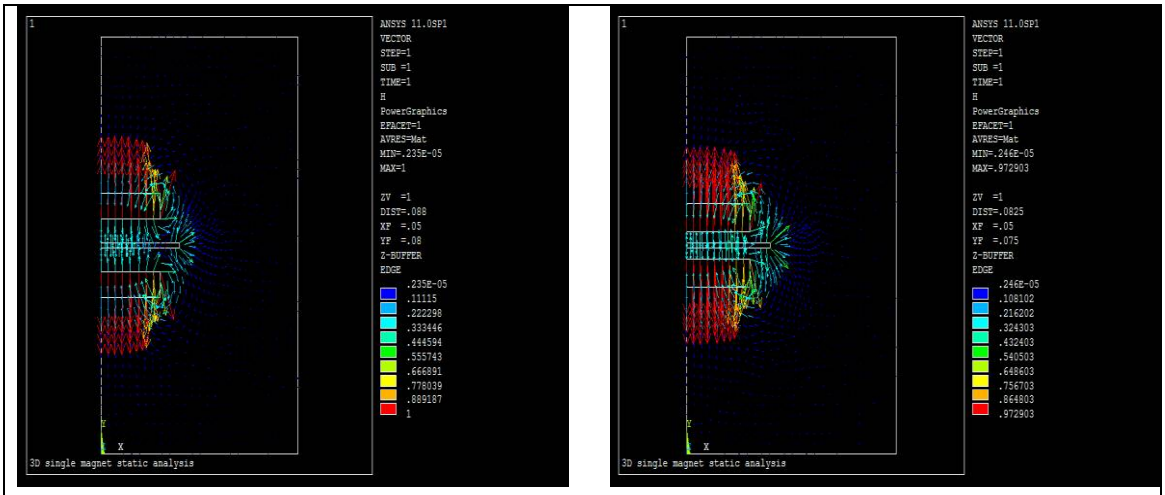

a: Field Intensity for X=20 mm **b: Field Intensity for X=10 mm**

Figure 4.14: Magnetic field intensity at gate center for different distance and t_2=2mm, μ_2=100k

It indicates that the magnetic field will be retained by the gate efficiently with high permeable value, the maximum approach distance of the piston will be reduced and hence a strong power stroke can be attained but at the same time, the force required to operate the gate will be higher.

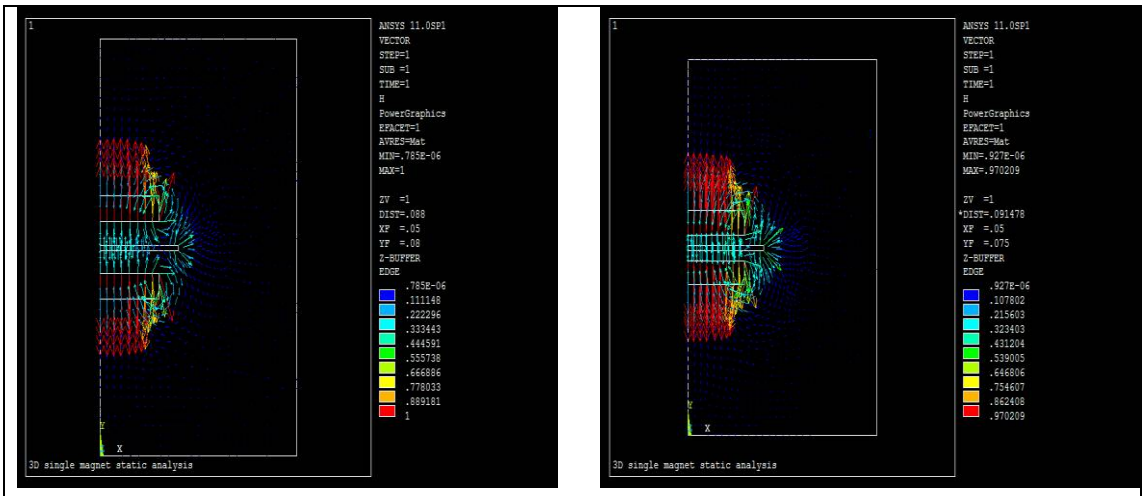

a: Field Intensity for X=20 mm **b: Field Intensity for X=10 mm**

Figure 4.15: Magnetic field intensity at gate center for different distance and t_2=2mm, μ_3=300k

The value of the field blocked by the gate decreases as the distance between the m_1 and m_2 increases. The variation in the field blocked by the gate with different location of the gate for μ_1=30k, μ_2=100k, , μ_3=300k, and for the distances of 20mm, and 10mm between the magnets is presented in the table 4.4.

Table 4.4: Magnetic field shielding for different values of μ for t=2mm

Sr. No	Distance/ Permeability	μ_1=100k	μ_2=100k	μ_3=300k
		Field blocked by gate (T)		
1	5 (mm)	0.44	0.83	0.95
2	10 (mm)	0.18	0.40	0.75

It can be concluded from the table 4.3 and table 4.4 that for various distance of the gate from m_1 and m_2, the shielding effect of the gate increases as the thickness of the shield material increases. The simulation value, run for different value of permeability and different distance for gate thickness of 1mm and 2mm, is summarized in the table 4.5. It can be concluded from the table 4.5 that the shielding effect of the gate increases as the thickness and permeability of the gate material increases. It is also observed that the distance between the m_1 and m_2 plays important role as the repulsive force between the m_1 and m_2 depends upon the air gap between

the gate and the magnets. High permeable with larger thickness material is highly effective for shielding purpose.

Table 4.5: Magnetic field shielding for different distances of the gate from m_1 andm_2

Sr. No	Permeability (μ)	Distance (mm)	Field blocked by gate for t_1=1mm	Field blocked by gate for t_2=2mm
1	30,000	5	0.23	0.44
		10	0.11	0.18
		15	0.03	NA
2	1,00,000	5	0.55	0.83
		10	0.24	0.40
		15	0.11	NA
3	3,00,000	5	0.77	0.95
		10	0.43	0.75
		15	0.21	NA

4.5 Dynamic Analysis of GOPI Engine

Dynamic analysis of the GOPI engine is performed in the ANSYS simulation 2D environment. Table 4.6, table 4.7 and table 4.8 represents the mechanical and magnetic properties with dynamic dimension of the GOPI engine.

Table 4.6: Mechanical properties of the GOPI engine

Particular	Geometry	Dimension
Bore	circular	Diameter=60mm
Stroke	I shaped	Length=139.7mm
Speed	10 RPM	

For dynamic analysis of the GOPI engine, the engine run for two different conditions, in the first condition the simulation was run when there is no gate between the m_1 and m_2 or the permeability of the gate is very less and in the second condition when high permeable shield gate is used. Gate material with thickness t=2mm, and permeability of μ=30 k is chosen for the simulation of the gate as μ=30 k is chosen for the gate development.

Table 4.7: Magneto -Mechanical properties of the GOPI engine

Particular	Geometry	Dimension
Fixed magnet and piston head magnet	Solid circular disc	Diameter=60mm Thickness=10mm
Gate	Circular-two paneled	Diameter=80mm Thickness=2mm

It is obvious to select 300k or higher permeable material for gate fabrication but, as high permeable materials are not available in the market for experiment purpose, so simulation was run with this permeable value of the gate.

Table 4.8: Magnetic properties of the GOPI engine

Particular	Type	Magnetic field intensity (H)	Permeability (μ)
Fixed magnet	NdFeB	1.2 T(-Y direction)	Relative μ=1
Piston head magnet	NdFeB	1.2 T (+Y direction)	Relative μ=1
gate	Hydrogen annealed		30,000

To run the simulation, symmetry effect along the stroke length of the engine is produced. For this the X=0, Y=0 (0,0) coordinates of the system is taken at center of the BDC of the magnetic piston. The Y coordinate of the system represent the position of the magnetic piston and the X coordinate system represent the position of the gate.

Y1,Y2 position of the magnetic piston from BDC

X1,X2 position of gate from axis of symmetry(Y axis)

X and Y Coordinates of magnetic piston and gate for rpm=10 is presented in the table 4.9. The total time taken by the magnetic piston to cover stroke length is divided into 5 equal parts for effective simulation and experimental study. The gate is synchronized with the piston movement in such a way that the gate will be in neutral position (fully inserted between the m_1& m_2 gap) when the piston is at TDC and the gate will be in active position (fully pushed out from the gap) when the piston is at BDC.

Table 4.9: The coordinates of the piston and the gate

Position of the piston	Ymp (X1,Y1)	Xgate (X2,Y2)
P_1	0,139.7	0,151.7
P_2	0,111.76	6,151.7
P_3	0,83.82	12,151.7
P_4	0,55.88	18,151.7
P_5	0,27.94	24,151.7
P_6	0,0	30,151.7

When less permeable material is chosen for the gate (μ=30k), the magnetic field lines of the magnets from both side of the gate will not be blocked properly and hence some counter magnetic force will remain there between the fixed magnet and the piston. This counter magnetic force between the m_1 and m_2 will reduce the speed of the piston when it approaches TDC.

As the piston moves down towards the BDC, the attachment of the m_2 with gate will reduce but repulsive force between the m_1& m_2 will increase. Initially, there will be huge repulsive force because of the magnetic poles uncovered but as the piston continuously moves towards BDC, the intensity of the repulsive force decreases. The gate is maintained to move outward with a constant rate.

The force available at piston head for various positions is presented in the figure 4.16. The magnetic force is maximum when the piston is at TDC even though no power stroke will happen there as, initially the gate will retain the force. As the piston start moving towards BDC from the TDC, the gate also starts moving outward in the x direction, uncovered the fixed magnet and the magnetic piston. The magnetic repulsive force between the magnets starts acting at the uncovered area and the thrust will be produced. During the continuous motion of the gate and the piston, more area of the magnets is exposed and hence more repulsive force between them occurs.

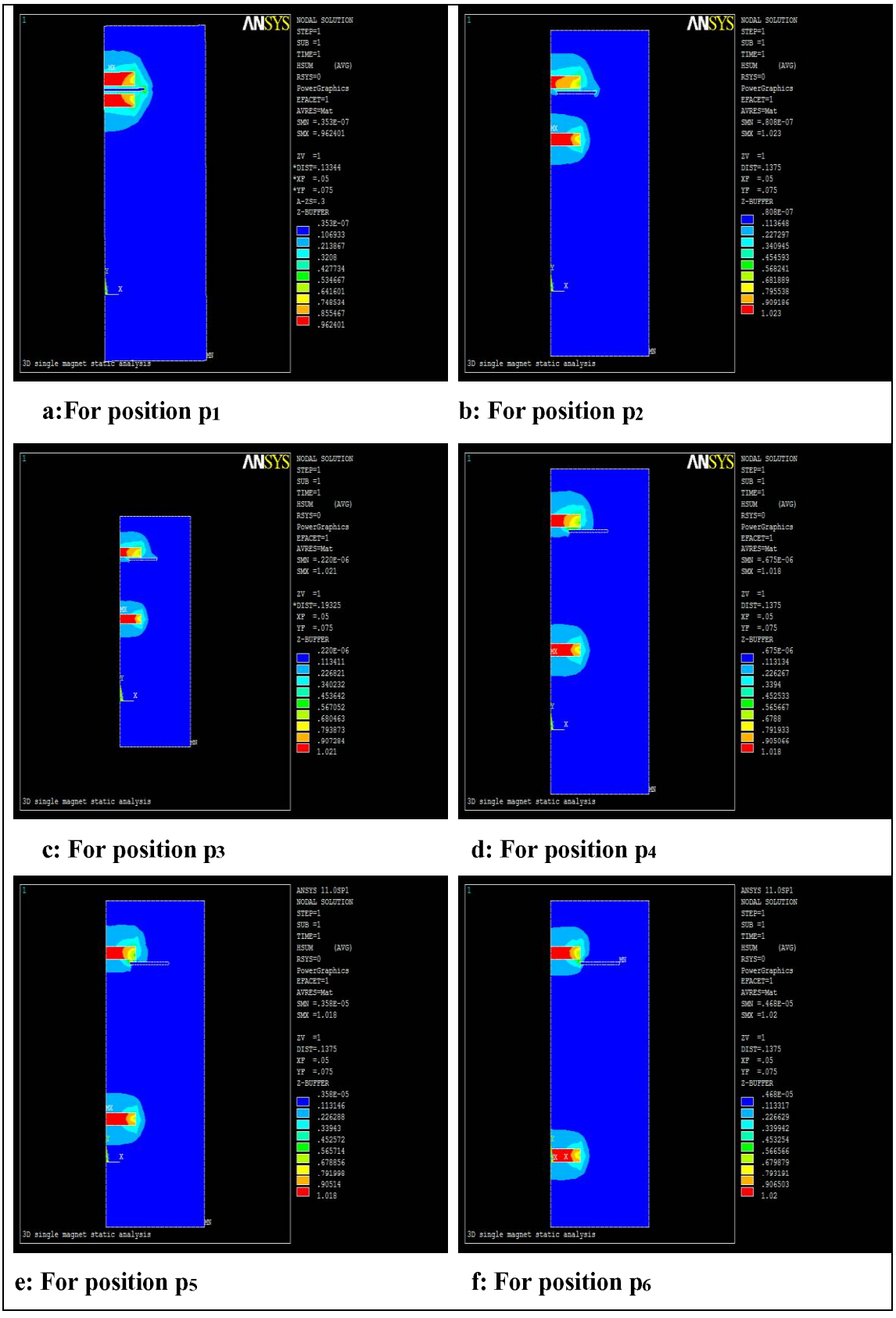

Figure 4.16: Force available at piston head for different position of piston

The magnetic circuit counter lines are presented in the figure 4.17. Initially, when the piston is TDC, the gate will be virtually attached with both the magnets, as presented in the fig 4.17 (a) and fig 4.17 (b). The magnetic inertia force to operate the gate at this position will be higher and hence more input will be required to operate it. As the piston moves downwards continuously, the attachment of the gate with piston declined as presented in the fig 4.17 (c) and fig 4.17 (d). The magnetic circuit consist only fixed magnet and the gate for the piston position p_5 and p_6. It means as the piston approaches nearer to BDC, the magnetic field lines of the m_2 does not affect the motion of the gate but the m_1 will strongly attached with it. So, it is obvious not to pull the gate completely out to expose the magnets for power stroke process but it is meant to operate in such a way that the area of the magnets can be partially uncovered where the flux density remains maximum.

Magnetic force between m_1&m_2 is almost zero when the piston is at BDC because of large distance between the m_1 and m_2. Force required to operate the gate at this position of the piston is only to manage the mechanical inertia of the gate hence the power required to operate the gate is minimum.

When the distance between the fixed magnet and the magnetic piston become more than their diameter (it is 60 mm in the above case), the repulsive force between the magnets will decrease rapidly. The magnetic piston (m_2) will be completely detached from the gate but the attachment of the m_1 with gate will increase, as shown in the figure 4.18. The intensity of the attachment of both magnets (m_1& m_2) with the gate will weaken as the gate keeps moving away from the axis of symmetry. It is obvious that the strong power stroke can happen when the piston is at TDC but it is also to be noted that the force required to pull the gate outward will be maximum at this position as shown in the figure 4.19.

The simulation for the force required to operate the magnetic inertia of the gate at the piston position p_6 was not run because beyond this position of the piston, there is no need to pull the gate outward as the repulsive force between the magnets will not contribute anymore in the stroke even the areas of the magnets uncovered fully.

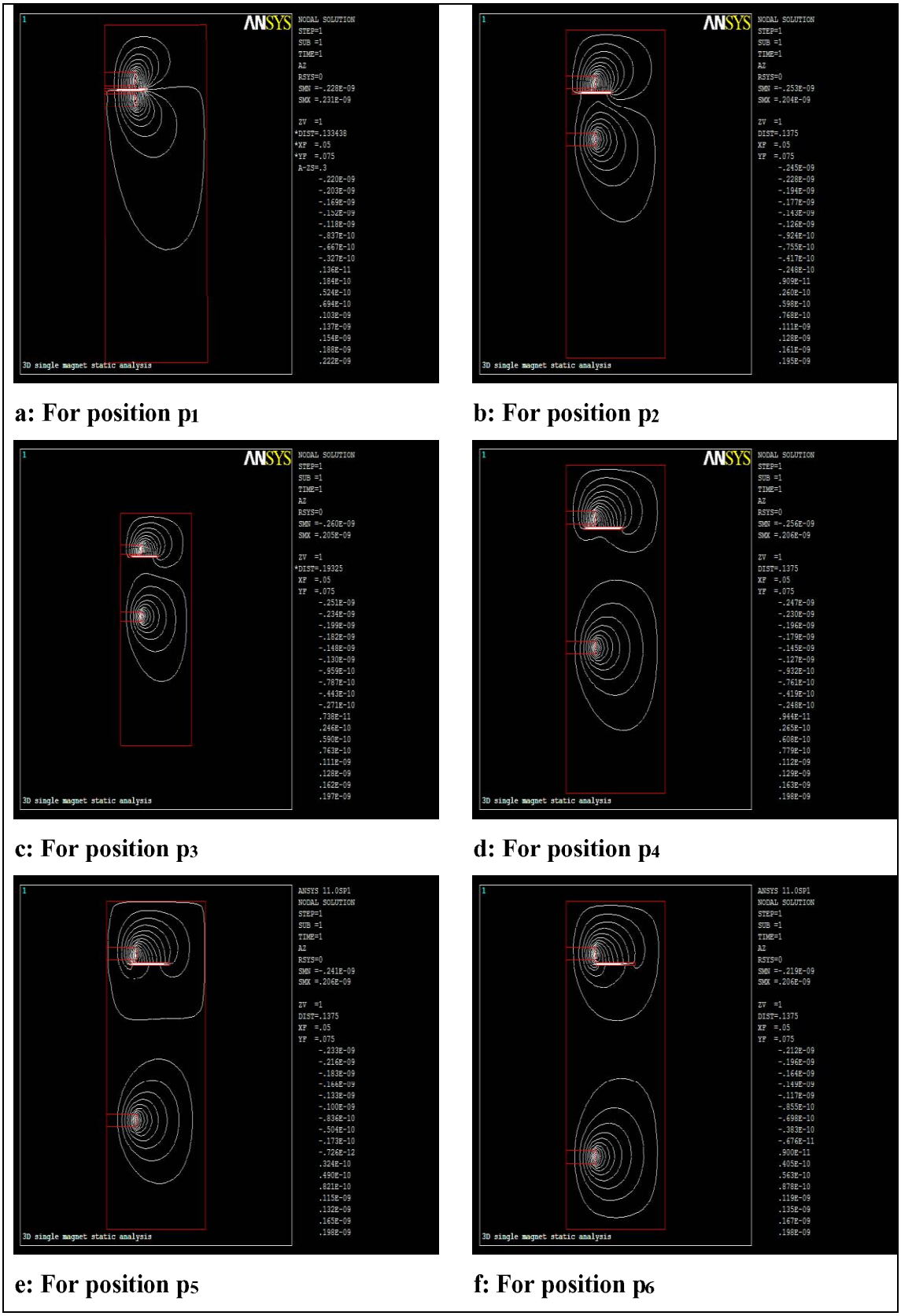

Figure 4.17: Magnetic circuit contour lines for different position of piston

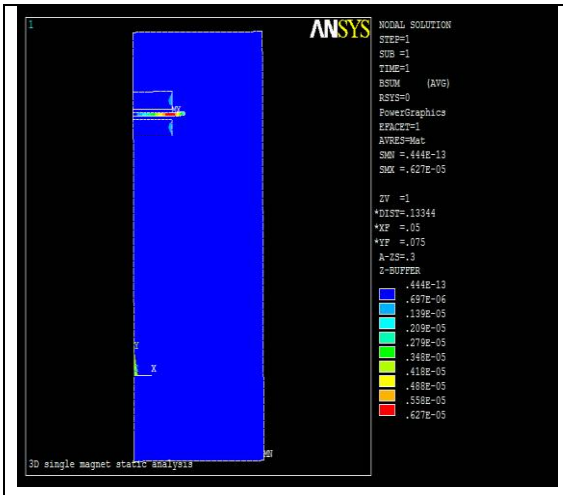

a: For position p_1

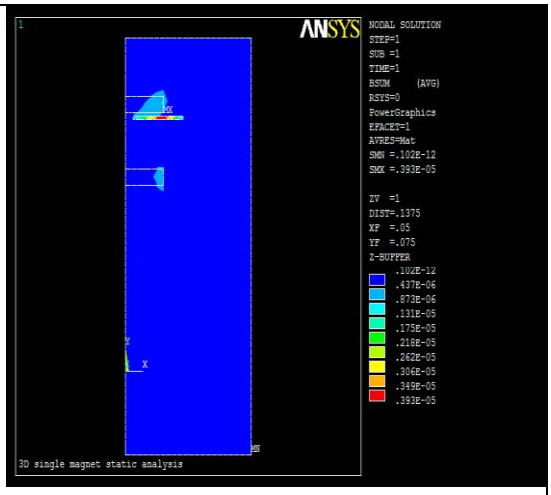

b: For position p_2

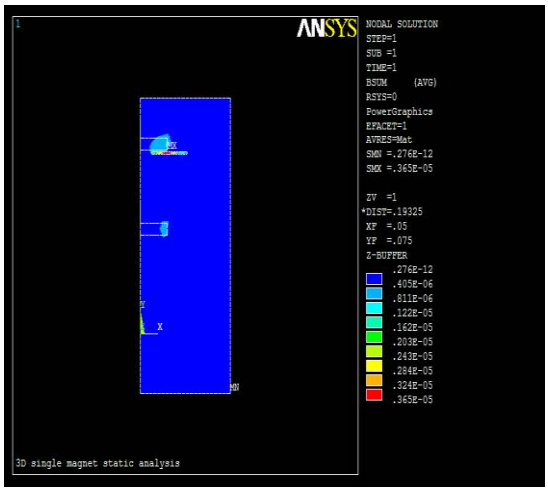

c: For position p_3

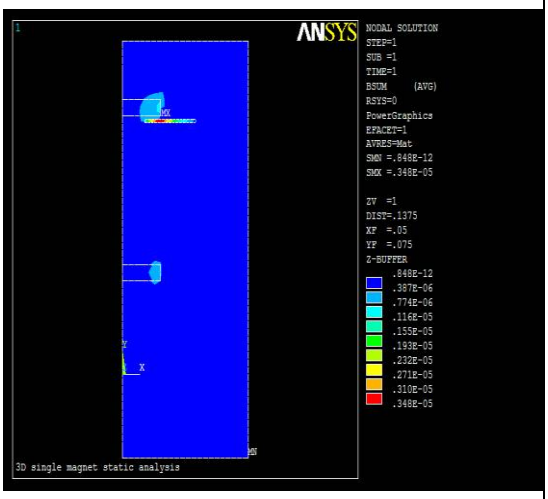

d: For position p_4

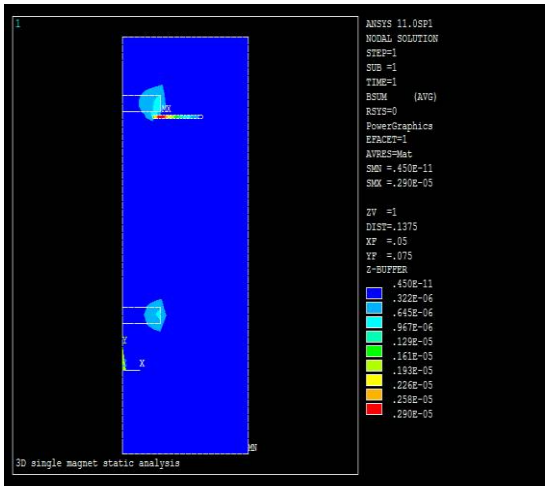

e: For position p_5

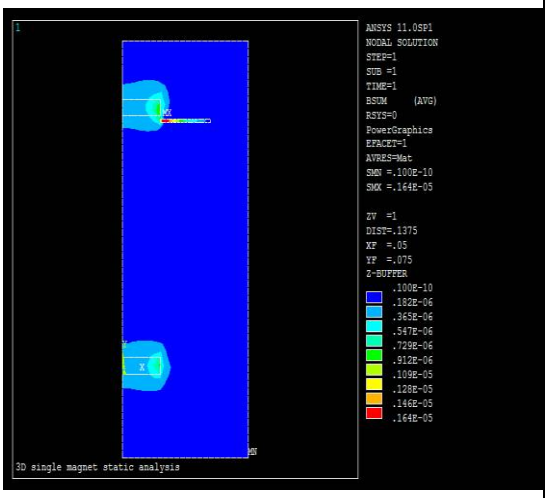

f: For position p_6

Figure 4.18: Magnetic field blocked by the gate for different position of the piston

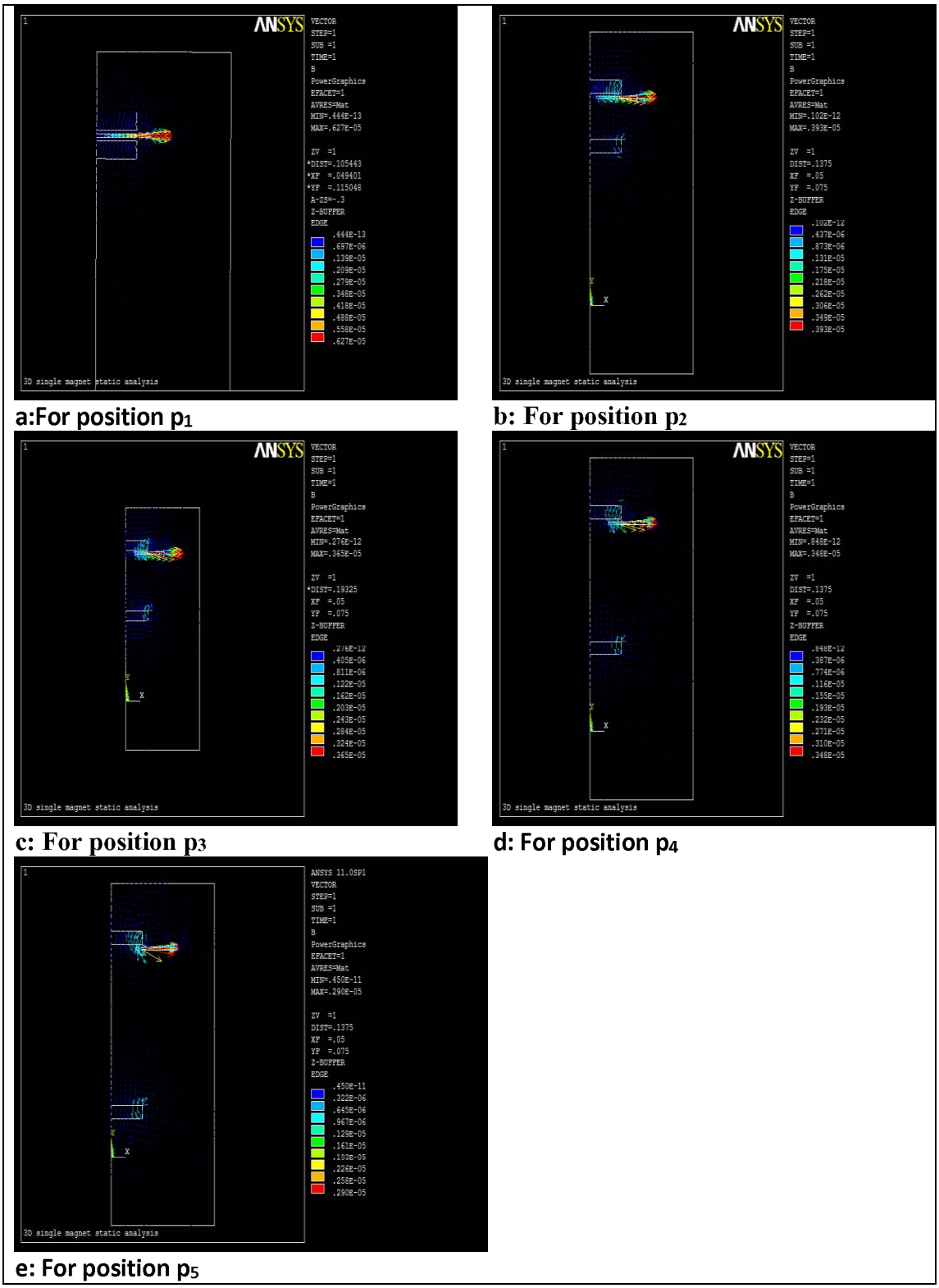

Figure 4.19: Force required to pull the gate for different position of the piston

To understand the behavior of the magneto properties of the engine closely, a simulation for μ_3=300k was also run.

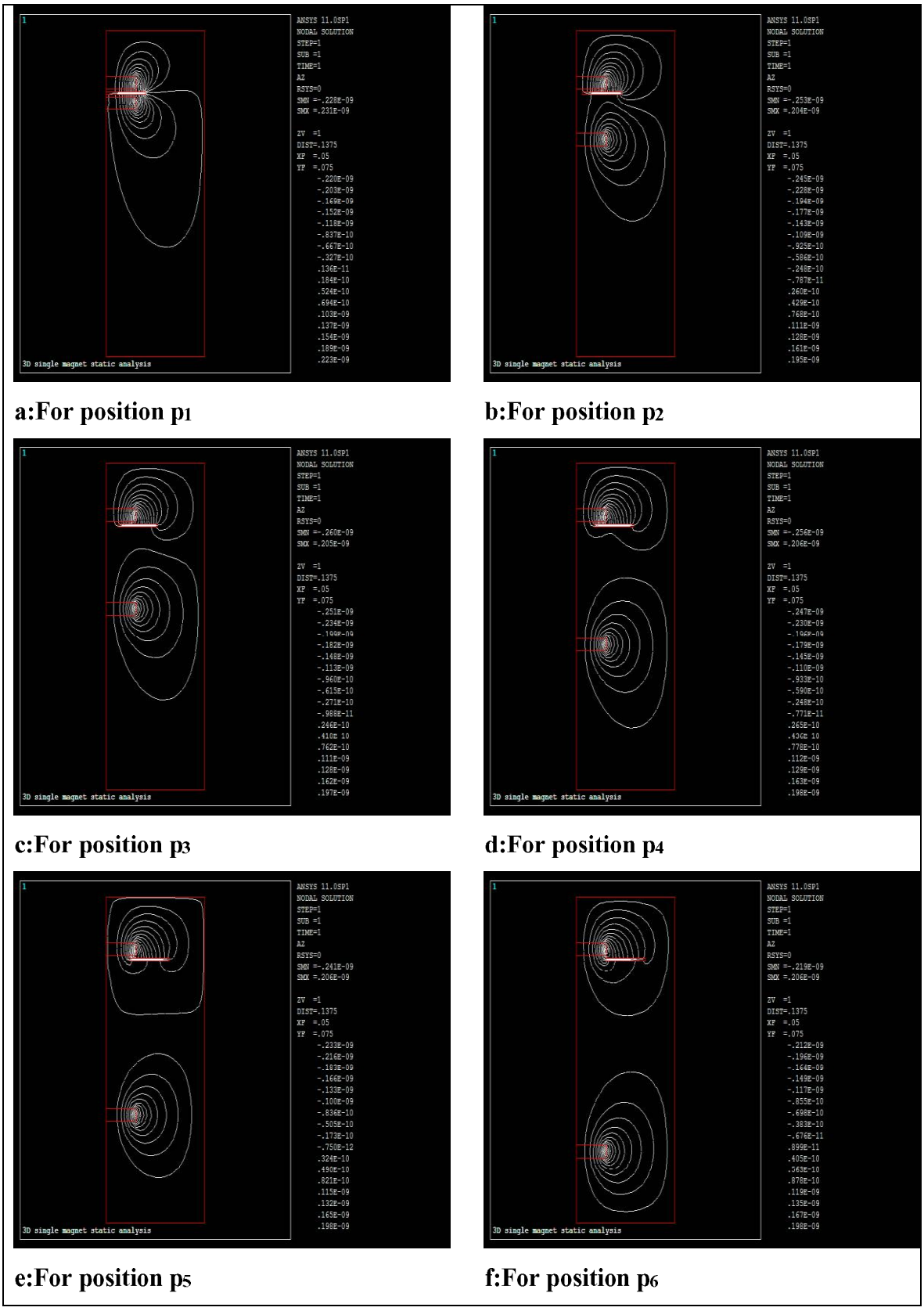

a:For position p_1 **b:For position p_2**

c:For position p_3 **d:For position p_4**

e:For position p_5 **f:For position p_6**

Figure 4.20: Magnetic circuit contour lines for different position of piston for μ_3=300k

For high permeable gate, the magnetic field lines attached strongly as maximum force is retained on the gate. As the piston moves down, the overlapping of gate with m_2 is reduced but m_1 is increased from both the side of it. The magnetic field lines start spreading across the gate because of two reasons (a) as the gate is moving away from the m_1, the magnetic circuit path length increases and (b) the distance between the m_1 and m_2 increases.

4.6 Efficiency of the GOPI Engine

Efficiency of the GOPI engine depends upon many parameters like selection of permanent magnets for magnetic piston and fixed magnet, shield material for gate, operating mechanism of the gate, distance of the gate from the m_1 and m_2. For this research report, a theoretical conclusion is drawn for the engine efficiency.

The Fm, the available magnetic force between the m_1& m_2, is a part of the net force on the piston head. Because of Fa, the virtual attachment of the m_1& m_2 with the gate and the Fag, the required force to counter balance the magnetic inertia of the gate, the efficiency of the engine is governed by the force component Fag which further depends upon the gate factor and the gate coefficients (b,d, p). So the working, as well as, the efficiency of the engine depends upon the basic properties of the permanent magnets and the shield material to be selected for the engine development as the gate coefficients depend upon magnetic flux density (B), distance between m_1& gate(x_1) and m_2& gate(x_2), permeability of the gate material (μ) thickness of the gate (t).

The coefficients b, d and p depends upon

- Magnetic flux density (B)
- Distance between m_1& gate(x_1) and m_2& gate(x_2) (x_1,x_2) (including air gap between m_1 and m_2 and the gate)
- Permeability of the gate material (μ)
- Thickness of the gate (t)

Mathematically, b, d and p depends upon these parameters as

$$(b, d, p) = f(B, \mu, t, x_1, x_2) \quad \textbf{(4.1)}$$

The dependency of the gate factor (a) on b, d, p can be explained as

$$a = k_1 * (b^{r1}) * (d^{r2}) * (p^{r3}) \quad \textbf{(4.2)}$$

And the magnetic inertia force, Fag as

$$Fag = k_2 * f(a,b,d,p, m) \quad \textbf{(4.3)}$$

Here, it is to be noted that when a=0; Fag ≠0 as some external force is required to pull out the gate from its neutral position. The power stroke of the engine not only depends upon the engine parameters like gate factor, gate coefficients, net force available at piston head but also on the gate geometry and the gate velocity with which the gate operates. Power in the stroke (Ps) can be explained by the equation as

$$Ps = k_3 * f(B, \mu, x_1, x_2, t, v, gg) \quad \textbf{(4.4)}$$

Here, gg is the geometry of the gate and v is velocity with which the gate operates.

Relation between the gate factor (a) and the magnetic inertia force (Fag)

$$Fag = k_4 * [f_1(a) * f_2(b, d, p)] \quad \textbf{(4.5)}$$

Relation between gate factor (a) and power stroke (Ps)

$$Ps = k_5 * (a)^{n1} * (gg)^{n2} * (v)^{n3} \quad \textbf{(4.6)}$$

Relation between efficiency (ɳ) and other parameters (a, Fag, Ps)

$$\eta = f((Ps, a, Fag) \quad \textbf{(4.7)}$$

Indirectly the ɳ depends upon f(b, d, p)

Or

$$\boldsymbol{\eta = f((Ps, Mp, Fnet)} \quad \textbf{(4.8)}$$

Schematic representation of the various component dependency of the GOPI engine

ɳ ⟶ Ps ⟶ Fag ⟶ a ⟶ (b, d,p) ⟶ f(**B, μ, t, x_1,x_2)**

Further, the GOPI engine parameters can be classified as per static characteristic and dynamic characteristic. The gate coefficients and gate factor are static in nature as once the material properties of the gate is defined it will not change during the operation of the engine. The magnetic inertia force, power stroke are dynamic characteristic of the engine as the value of these parameters varies continuously.

b, d, p = **static characteristic**

a = **static characteristic**

Fag = **Dynamic characteristic,** which further depends upon mass of the gate (gate mechanical inertia)

Ps = **Dynamic characteristic** which further depends upon geometry of the gate, velocity of the gate opening and closing

Here;

k_1, k_2, k_3, k_4, k_5, k_6, r_1,r_2,r_3, n_1, n_2, n_3 are constants

The value of the constants can be finding out by conducting experiments on the GOPI engine. Theoretical relation between the engine parameters based on mathematical modeling are presented in the table 4.10 and table 4.11.

Table 4.10: Theoretical relation between the GOPI engine parameters (d=0)

Sr. No	d	b	p	a	η (efficiency)
1	0.0	0	1	=0	η =0
2	0.0	0.25	0.75	1>>a>0	η ˜0 but η>0
3	0.0	0.5	0.5	1>a>0	1>>>η>0
4	0.0	0.75	0.25	1>a>0	1>>η>0

It can be concluded from the table 4.10 and table 4.11 that the maximum efficiency of the engine is when the gate coefficient d is equal to 1, its maximum value and the b and p coefficients equal to zero. The virtual attachment between the magnets and the gate does not exist and the required input power to operate the gate is minimized. But it is also to be noted that when the gate factor is one for different values of the b and d coefficients, the efficiency varies accordingly.

Table 4.11: Theoretical relation between the GOPI engine parameters (d≠0)

Sr. No	d	b	p	a	η(efficiency)
1	0.0	1.0	0.0	a=1	1>>η>>0
2	0.25	0.75	0.0	a=1	1>η>>0
3	0.5	0.5	0.0	a=1	1>η>>>0
4	0.75	0.25	0.0	a=1	1 ˜ η>>>0
5	1.0	0.0	0.0	a=1	η=max

4.7 Validation of Mathematical Modeling and Simulation Results with Experimental Outcome

In working condition of the engine (when f=0, where f is counter force) the repulsive force between the fixed magnet and the magnetic piston is zero when the piston is at TDC but as the piston starts moving downward from TDC towards BDC, the repulsive force between the m_1& m_2 start acting. The effective area where power stroke happens; increases as the gate moves away from the neutral position. Initially, the force on the piston head is zero, but starts increasing sharply as the distance between m_1 and m_2 decreases. Whereas, when the piston keeps on moving downwards, the distance between the m_1 and m_2 increases and the force between them starts to decrease. It can be observed from the table 4.13 that magnetic force with very high intensity is available only for very short range from the magnets.

A manually operated GOPI engine is designed and developed to observe experimental results. The material used for fabrication, their geometry and dimension taken for GOPI engine development are described in detail in the section 3.3 of the chapter 3 under the heading development of the engine components.

In the fig 4.21 the fixed magnet embedded in the wooden cylinder is shown. The metallic sheet is the gate which is capable to shield the magnetic field from one side. This gate is used to slide over the engine track to produce the magnetic power stroke. The movement of the gate and magnetic system is synchronized in such a way that when the gate removed completed from the neutral position, the magnetic piston head will reach to BDC.

Figure 4.21: Fixed magnet and wooden cylinder with gate

In the fig 4.22, a complete embodiment of the GOPI engine is presented. The gate is manually operated. The magnetic piston moves up and down in the reciprocating motion. This motion is converted into rotational motion by the crank assembly. The engine is run under no load condition as the main objective of the experimental investigation is to observe the magnetic behavior of the magnets m_1 and m_2 with the movement of the gate.

It is observed during the experiments that when the fixed magnets are covered with shield material from one direction (facing piston head) maximum approach distance of the piston is increased by 2-3 mm (distance between the fixed magnet and the magnetic piston is reduced) and when the fixed magnet is covered through all the sides, the maximum approach distance of the piston is increased by 5-6 mm which validates the mathematical modeling and simulation result that if the magnetic field is blocked by the gate, the distance between the fixed magnet and the magnetic piston will be reduced and more power will be attained in the stroke.

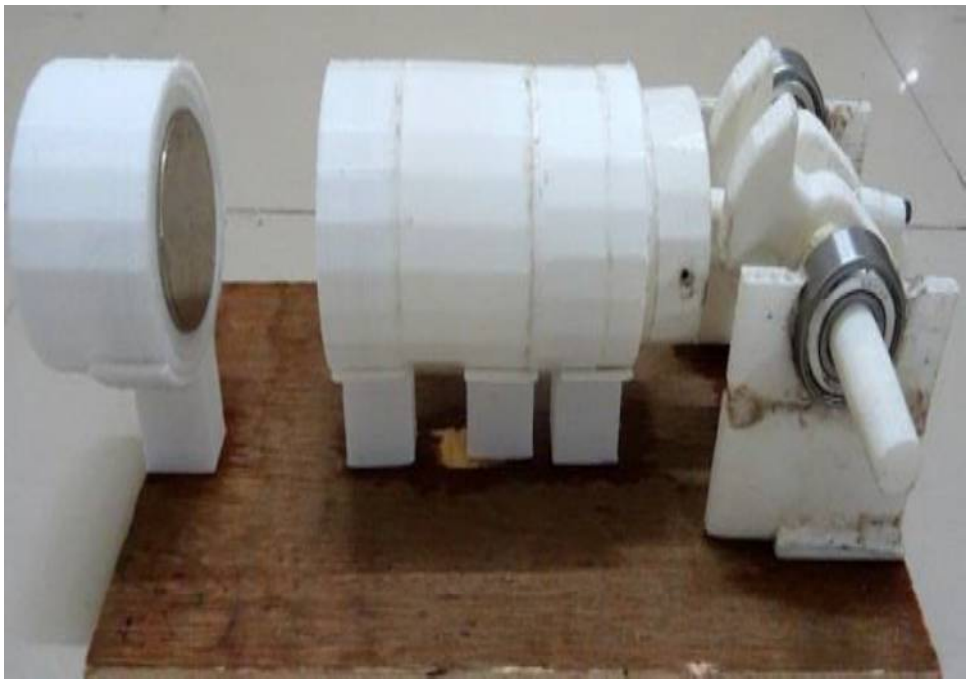

Figure 4.22: Complete embodiment of the GOPI engine

The value of the magnetic thrust decreases sharply in two conditions: it decreases when the distance between the magnets increases and secondly it decreases as the radial distance from the center of the magnet increase. It is observed that maximum magnetic thrust occurs at the center of the magnets and its value falls down sharply in the radial outward direction.

Table 4.12: GOPI engine parameters

Sr. No	Particular	Units	Dimension
1	Bore(mm)	mm	60
2	Stroke Length	mm	139.7
3	Speed	RPM	10

It is observed during the experiments that there is maximum magnetic thrust when both the magnets are close enough and it occurs mainly at the center of the magnets.

Table 4.13: Force at piston head for different piston position (from TDC to BDC)

Sr. No	Force between m_1&m_2 (area =A) (N)	Effective area (m)(A/5)	Effective Force (N)=Fm
P_1	625324	0.0	0
P_2	5101	565.2	1020.2
P_3	677	1130.4	270.8
p_4	179	1696.5	107.4
P_5	66	2261	52.8
P_6	35	2826	35

It is observed during the experimental investigation that pulling out the gate from the neutral position required huge force. Sometimes the synchronization between the magnets and the gate movement is mismatched and the engine stops working as the magnetic piston get stuck in its way.

Table 4.14: Effective force at piston head moving from TDC to BDC

Sr. No	Piston position (mm) (Y)	Gate position (mm) (X)	Force between m_1&m_2 (N)	Effective area (m)(A/5)	Effective Force (N)=Fm
P_1	0.0	0.0	625324	0.0	0.0
P'_1	5.59	1.2	139090	113.04	27818
P'_2	11.18	2.4	40974	226.4	16389
P'_3	16.76	3.6	17899	339.12	10739
P'_4	22.35	4.8	9100	452.16	7280
P_2	27.94	6.0	5101	565.2	5101

Here, the $p'_1$to p'_4 are intermediate positions between the p_1 and p_2.It is also observed during the experiments that as the magnetic piston moves away from the TDC, the attachment of the m_1 with the gate increases. This attachment of the gate with m_1 required extra force to pull and push the gate on the engine track. Because of this

attachment, the engine efficiency decreases. The experimental observation and simulation results match and support each other. The calculation of exact force at piston head and force required to pull the gate from neutral position and other parameters required a detailed experimental investigation.

Table 4.15: Attachment of gate with m_1& m_2 for different position of the piston

Position of the piston	Force at piston head (N)	Attachment of gate with m_1&
P_1	0 (gate in closed position)	m_1& gate-full attachment & gate-full attachment
P_2	1020.2	m_1& gate- attachment>70% & gate attachment>30%
P_3	270.8	m_1& gate- attachment>70% & gate attachment~0
P_4	107.4	m_1& gate- attachment>70% & gate attachment=0
P_5	52.8	m_1& gate- attachment>70% m_1 will start attaching gate from bottom side > 20% & gate attachment=0
P_6	35	m_1 & gate- attachment>70% m_1 will start attaching gate from bottom side > 50% & gate attachment=0

According to the mathematical modeling developed and discussed in the section 3.5 of the chapter 3 under the heading mathematical modeling, the equation 3.4, equation 3.5, equation 3.7 supports the simulation results and experimental observations.